Structural Characteristics of Developing *Nitella* Internodal Cell Walls

BY PAUL B. GREEN, PH.D.*

(From the Institute of General Botany, Swiss Federal Institute of Technology, Zurich, Switzerland)

PLATES 247 AND 248

(Received for publication, May 10, 1958)

ABSTRACT

The *Nitella* internodal cell is formed by a division of the segment cell, the latter being a direct derivative of the shoot apical cell. The internodal cell is remarkable in that it elongates from an initial length of about 20 microns to a mature length of about 60 millimeters. The structures of the apical and segment cells, and the internodal cells in all stages of development were examined with the techniques of interference, polarization, and electron microscopy. The apical and segment cells were found to be isotropic. The upper part of the segment cell, destined to form a node, shows a curious pitted structure that was characteristic of certain node structures. The lower part of the segment cell, destined to become an internodal cell, shows a vague transverse arrangement of fibrils at the inner wall surface. The internodal cells, from the time they are first formed, show negative birefringence and a transverse arrangement of microfibrils at the inner wall surface. The elongation of the internodal cell is characterized by a rise, dip, and rise in both the optical thickness and retardation of the cell wall. The dip in both these variables coincides with the attainment of the maximum relative elongation rate. After the cessation of elongation, wall deposition continues, but the fibrils at the inner surface of the wall are now seen to occur in fields of nearly parallel microfibrils. These fields, with varying fibrillar directions, may partly overlap each other or may merge with one another. Unlike the growing wall, this wall which is deposited after the end of elongation is isotropic.

INTRODUCTION

Stems, roots, coleoptiles, and other cylindrical plant organs elongate primarily through the extension of cylindrical cells in the direction of the organ axis. Many investigations of this directed extension have revealed an important correlation with cell wall structure: *e.g.* the cellulose microfibrils of an elongating cylindrical wall lie predominantly at right angles to the axis of the cylinder (as hoops on a barrel). This transverse position of microfibrils, "tubular texture," has been found in a wide variety of higher plant tissues (1), and in the large cylindrical cells of the alga *Nitella* (2). The correlation between cell form and fine structure of the cell wall will here be examined in detail in developing *Nitella* internodal cells. All phases of this "giant" cell's wall development, from its initiation (length, 20 microns) until its maturity (length 5 to 6 cm.) have been studied with interference, polarization, and electron microscopy. The first two techniques yield quantitative data which may be related to the elongation rate of the cell. The last mentioned method gives a high resolution image of the inner surface of the wall where wall formation is going on (3).

The *Nitella* plant consists of successive nodes and internodes (Text-fig. 1). The nodes are multicellular and contain the laterals of limited growth ("leaves") and of unlimited growth ("branches"). The internodes are large single cylindrical cells. All these structures stem from the activity of a single dome-shaped apical cell at the tip of the shoot (Text-fig. 1). About every 3 days this cell forms a cross-wall, parallel to its base, cutting off a segment cell (4). The segment cell then also

* Present address: Department of Botany, University of Pennsylvania, Philadelphia, Pennsylvania.

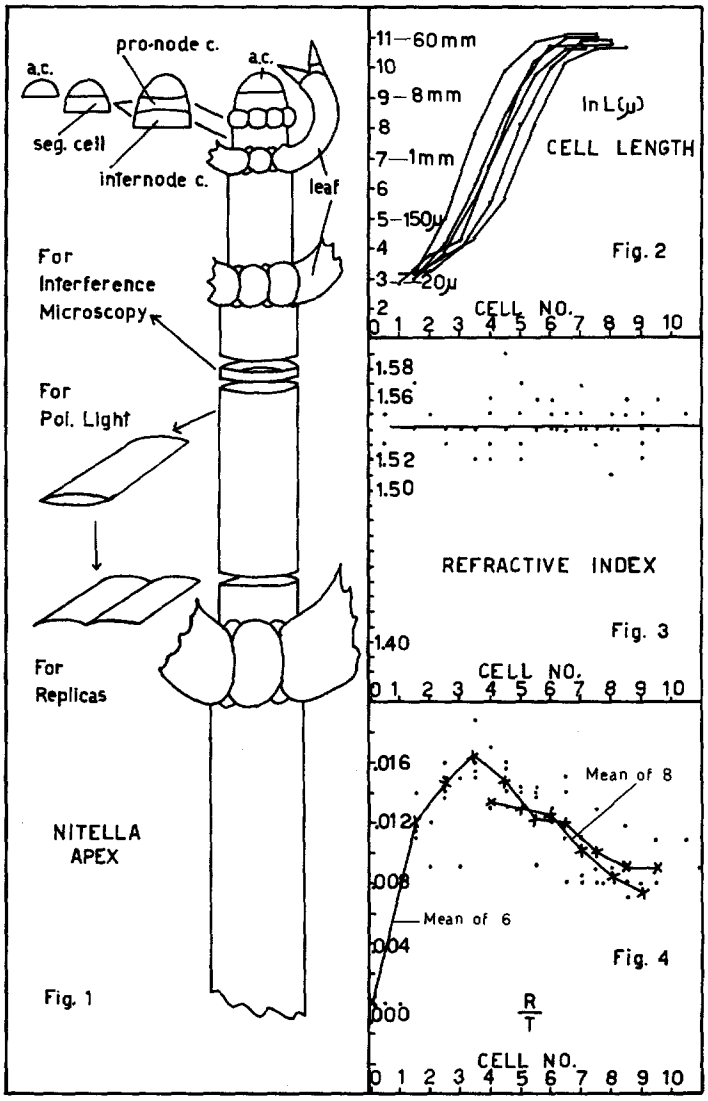

TEXT-FIGS. 1 to 4. TEXT-FIG. 1. Diagram of the *Nitella* shoot apex showing, at upper left, how the apical cell (*a.c.*) divides to form a segment cell (*seg. cell*), which in turn divides to form an upper pro-node cell and a lower internodal cell. The preparation of the cell wall for study in the interference, polarization, and electron microscopes (replicas) is sketched. TEXT-FIG. 2. The ordinate is the natural logarithm of cell length when cell length is measured in microns. Beside some of the logarithms stand absolute cell lengths. The abscissa is cell number, internodes being numbered from the shoot tip. Cell number is equivalent to age if multiplied by 3 days. TEXT-FIG. 3. Refractive index (ordinate) plotted against cell number. TEXT-FIG. 4. Retardation (R) divided by optical thickness (T) plotted against cell number. The curve *Mean of 6* is derived from the points shown. The curve *Mean of 8* is the mean data from 8 other shoots; the points are not shown. Changes in R/T reveal changes in either the orientation of the wall's birefringent material or the percentage of birefringent material, or both.

undergoes a transverse division; the upper cell formed is a pro-node cell which divides further to produce node structures, the lower cell is an internodal cell which will expand enormously to form part of the plant axis. The expansion of the internodal cell surface can be as large as 15,000 ×, the increase in cell wall volume may reach 30,000 ×.

Both the elongation and the increase in diameter of the internodal cell are evenly distributed along the cell axis (5). In accord with the uniform dis-

tribution of growth, the structure of a given cell wall is similar in all regions except for two very thin strips, "striations," which are formed where the ascending and descending streams of protoplasm slip past each other (2).

Because internodal cells are produced at about 3-day intervals by the segment cell, successive internodes differ in age by 3 days. This interval is called a plastochron (6, 7). In the present research an entire shoot was killed at once and all the internodal cells examined. The internodes were numbered, starting with the smallest, most apical, one and numbering toward the base. For the purpose of comparing different shoots, it is important to know whether the smallest internode has just been formed or whether it was produced several days ago and is about to become the second most apical internode through the division of the segment cell above. In Text-fig. 1 it can be seen that a just formed internodal cell at first has a pro-node cell and an apical cell above it. After some time (about 1½ days), the pro-node cell has divided several times and the apical cell has produced another segment cell. These two events occur about in the middle of the plastochron. When the smallest internode was under just a pro-node and apical cell, it was given number 1 and all older internodes were designated by whole numbers. When the smallest internode appeared under a developing node, segment cell, and apical cell, it was given number 1½ and all older internodes were numbered 2½, 3½, etc. Thus data from various plants could be plotted against cell number with an accuracy of one-half plastochron.

Experimental Methods

A clone of *Nitella axillaris* Braun was used throughout. Cultures were grown in an autoclaved medium of 2 per cent garden soil in distilled water. One preparation of medium supported rapid growth for up to 1 month. In the present study the techniques of light and electron microscopy were used to examine the development of the internodal cell, beginning with its formation from the apical and segment cells. This methods section will be long because the techniques of the two types of microscopy are different and, further, because special preparative methods had to be developed to permit study of the small cells at the plant apex. An additional subdivision of this section concerns the presentation of growth data.

Growth Data.—It is rewarding to present the structural data not only in relation to cell number (age), but also in relation to cell length and especially cell elongation rate. Elongation is evenly distributed along the cell axis and for this reason the relative rate of elongation, which takes cell size into account, is the most convenient measure of growth. For example, a *Nitella* cell elongating from a length of 5 mm. to one of 10 mm. during a plastochron (3 days) would be displaying relatively more growth activity than one growing from 45 mm. to 50 mm. during a plastochron. In this example the absolute elongation rate, dL/dt, is 5 mm./plastochron for both cells, but the relative elongation rate, $1/L\ dL/dt$, is much greater for the smaller cell. The relative rate of elongation is the absolute rate of elongation divided by cell length, and it could be determined directly with *Nitella* if it were convenient to measure the elongation rate and cell length accurately and quickly just before killing the cell. This was found impractical and the relative elongation rate was estimated from measurements of lengths of consecutive internodes in the plant axis as described below.

The relative rate of elongation, r, is equal to the value of the exponent in the equation of exponential growth:

$$L = L_1 e^{r(t_2 - t_1)}, \tag{1}$$

in which L_1 is initial length, L, the length at the end of the time period $(t_2 - t_1)$. If natural logarithms are taken of (1) and the equation differentiated with respect to time, t, one finds

$$\frac{1}{L}\frac{dL}{dt} = r. \tag{2}$$

In a cell with elongation evenly distributed along the axis, the cell may be considered to be growing exponentially because the rate of increase in length is a function of length. If the rate of exponential elongation were constant, then r would need to be determined only once. In the developing *Nitella* internode, however, the relative rate of elongation is not constant and in this study the rate was determined for each internode in each shoot studied.

The relative rate of elongation is often estimated by the formula

$$r = (\ln L - \ln L_1)/(t_2 - t_1). \tag{3}$$

The analogous formula, giving the mean relative rate of elongation per plastochron, p, is

$$p = \ln L_n - \ln L_{n-1}, \tag{4}$$

in which L_n is the length of internode n and L_{n-1} the length of the next younger one. This formula has the disadvantage that it gives the mean rate during a period of one plastochron (the previous plastochron for cell n, the plastochron to come for cell $n - 1$). The relative rate at the time of killing the cell is estimated by a formula (Erickson, letter) which gives, for cell n, the mean of two rates, the rate during the previous plastochron (since cell n was the size of the present cell

$n - 1$) plus the rate during the plastochron to come (until cell n has the present size of cell $n + 1$):

$$p = \tfrac{1}{2}(\ln L_{n+1} - \ln L_{n-1}). \quad (5)$$

This equation may be formulated by a second method. When the natural logarithm of cell length is plotted against plastochron age, the slope at any point on the curve is equal to the relative rate of elongation, whether the curve is straight or not. Equation (5) gives a close approximation for this slope by numerical differentiation, for the point (n, $\ln L_n$), based on the fitting of a parabola to the three points ($n - 1$, $\ln L_{n-1}$), (n, $\ln L_n$), and ($n + 1$, $\ln L_{n+1}$) after Milne (8). Deriving equation (5) in this way involves no assumption of steady exponential elongation (linear semilog plot of length against plastochron age) for the estimation of the relative rate of elongation. The determination of p by equation (5) for developing *Nitella* internodes reveals a characteristic single peaked curve which shows a correlation to changes in certain wall properties (Text-figs. 5 to 10).

Light Microscopy.—It was desired to measure optical thickness, retardation, and refractive index for the walls of the apical and segment cells and all the internodal cells of the shoot. Optical methods require cytoplasm-free thicknesses of cell wall. Such preparations were easy to make with internodes longer than 1 mm. The cells were cut at their two ends, isolating the cylindrical portion. To remove the protoplasm this piece was stroked, under water, with a hair loop fixed to a rod. These flattened cylindrical pieces of wall (Text-fig. 1) were examined in a polarized light microscope and the retardation of the double thickness of wall was measured with a Berek compensator. Use of a double thickness is permissible because previous work (2) has shown that superposition of the two sides of the cylinder results in no cancellation of retardation. Use of double thicknesses gave increased accuracy to the measurements.

For the measurement of wall optical thickness, a short segment of the collapsed cylinder was removed by cutting (Text-fig. 1), and this piece was placed on a glass slide along with other similar pieces from the same shoot. These segments came from pieces of wall whose retardation had already been determined. The segments were arranged in order of increasing cell number (age). Preliminary work had shown that wall thickness within a given wall was essentially constant, so a small piece could be taken as representative of the whole wall. It was possible to photograph, simultaneously, parts of a whole series of internodes (Fig. 2), each piece being 3 days older than the one above. In the Dyson interference microscope the field can be so arranged that it is crossed by a system of parallel dark bands; the distance between bands represents an optical path difference of one wave length. When the object is inserted into the field, the bands are still apparent, but they are displaced in the region of the object (Figs. 1 *b* and 2). The extent of this displacement, when divided by the distance between bands, gives, in wave lengths, the optical path difference between a path through the object and one through the medium of the mount. In a study of objects of uniform optical path difference, such as *Nitella* cell walls, it is necessary to identify a displaced band in the object with the corresponding one in the field. This is done when the field is illuminated with white light and the bands are transformed into a symmetrical system of Newton's colors. Thus the first order gray band of the field can be identified with the one in the object. The optical path differences, for double thicknesses, never exceeded one wave length. Negatives taken when the field was illuminated by monochromatic light (Na line about 5900 A) were analyzed in a Walker recording densitometer. The sine curve of light intensity was displaced in the object and from this displacement the optical path difference (O.P.D.) was calculated.

Optical path difference is equal to the optical thickness of the object (t) multiplied by the difference in refractive index between the object and the medium:

$$O.P.D._w = t(n_{obj} - n_{water}), \quad (6)$$

in which the O.P.D. is measured in water, and n is refractive index. This equation has two unknowns, n_{obj}. and t. These can be determined after the same preparation has been studied in a second medium with a refractive index different from that of water. Glycerin (n is 1.469) was used as the second medium. The penetration of glycerin into the wall was checked by comparing values of the optical thickness of small pieces of the same wall immersed in air, water, glycerin, dioxane, amyl acetate, acetone, and CS_2. Values were essentially identical in all cases. With the second medium one obtains a second equation with the same two unknowns:

$$O.P.D._g = t(n_{obj} - n_{glycerin}). \quad (7)$$

Equations (6) and (7) are combined to give a solvable equation for the refractive index of the object:

$$n_{obj} = \frac{O.P.D._w n_{glycerin} - O.P.D._g n_{water}}{O.P.D._w - O.P.D._g}. \quad (8)$$

A similar, more general equation appears in a paper by Barer (9). The refractive index of the object can be substituted in equation (6) to give the optical thickness of the object. Optical thickness is not the distance between the two surfaces of the wall but is the distance, within the cross-section, occupied by solid material (not penetrated by the medium). Optical thickness is proportional to mass per unit area and is independent of the state of swelling of the wall or its porosity. In this study thickness, t, refers to *optical thickness.*

For the study of internodal cells shorter than 1 mm. and of the apical and segment cells, the optical methods were the same in principle but only single thicknesses

were used and, of course, the walls were too small to contain more than one interference band for measurement (Fig. 1 *b*). Study of the apex is made difficult by the smallness of the cells of interest and the fact that the apical cell is hemispherical, not cylindrical. Further, the presence of small leaf cells which arch over the apex complicates the making of a flat preparation in which all the walls of interest are free from overlapping leaf cell walls. This latter is essential for optical measurements. The procedure developed was tedious and low in yield but it did give sufficient preparations of quality (Figs. 1 *a* and *b*) for an analysis of the apex. All the leaves of the apex were removed by puncturing them with a very fine needle and then ripping them free of the axis by pushing them toward the apex of the shoot. This operation was done in a large drop of water on a glass slide under a dissecting microscope. The apex, now consisting of internodal cells separated by small node cells and torn leaf bases, was made less firm by puncturing the internodal cells. A razor blade was then used to make a longitudinal cut splitting all the cells of the apex, including the apical cell, into two symmetrical halves. Each half-apex was similarly split, giving four "quarter-apices." The apical cell, originally a hemisphere, was thus cut into four pieces each of which could be flattened out with only a little distortion. Optical measurements were made as above.

Replica Procedure for the Electron Microscope.—As for the studies with light microscopy, slightly different procedures were used for larger (longer than 1 mm.) and smaller cells. The larger cells were cut and cleaned as described above and the collapsed cylinders were allowed to dry on the slide. A razor blade was used to make a longitudinal cut near one of the marginal folds of the wall. The narrow piece thus cut off was discarded and the larger piece, after wetting, was unfolded to give a single flat thickness of wall, inner surface upward. It was then dried. The wall and slide were shadowed with chromium at an angle of 45°. A thin layer of carbon was then evaporated normally onto the surface. The separation of the replica from the wall involved first the removal of the preparation from the slide. This was done by trimming the edges of the wall with a razor blade and placing a large drop of 20 per cent H_2SO_4 over the preparation. The acid penetrated the wall and weakened it during several hours. The slide was then immersed in a Petri dish of water and the preparation was teased free of the slide and made to float on the water surface, carbon side up. It was then transferred to the surface of a concentration series of H_2SO_4 (40, 50, 55, 60, 65, 75, 85, 100 per cent), floating about 10 minutes on the surface of each solution. The pretreatment in dilute acid so weakened the wall that the swelling of the wall in strong sulphuric acid did not tear the replica but rather helped separate the wall from the replica, giving quantitative removal of the wall. After floating on distilled water, the replica was placed directly on the specimen grid without a supporting film.

Replicas of the plant apex were made of the inner surfaces of apices "quartered" as described above. Because such preparations are much rougher than the large internode wall surfaces, a special method was needed to prepare an intact replica. The quartered apex was moved, under water, until it rested on the surface of a previously prepared flat piece of internodal cell wall. This wall served as a carrier. The preparation was shadowed as above, but the carbon was applied while rotating the specimen in the evacuated bell jar, depositing carbon from as many directions as possible. This attempted to make the carbon layer continuous, despite the roughness of the specimen due to torn edges of leaf bases, slight curvatures of the walls, etc. After removal from the bell, a small piece of paraffin wax was placed on the preparation and melted. The excess was drained off by tilting the hot slide; the apex was kept visible through a thin layer of solidified wax. The wax served to hold the replica together while the wall was being removed. While still on the glass slide, the carrier wall was trimmed and the surrounding wax scraped away. The specimen then was treated with acids as described above. After washing, the wax-covered replica was allowed to dry on a formvar-coated grid. Just before drying, the wax surface was held by a hair fixed to a rod so that the quartered apex rested over a large and long slot in the grid. Thus the small cells at the tip of the apex could be observed without interruption by a cross-bar of the grid. The final step was the removal of the wax with benzene.

RESULTS

After a brief mention of certain optical properties common to all developing internodes, various stages in internodal cell wall development will be described in greater detail, bringing in the results of electron microscopy.

Optical Investigation, General.—Of all the optical properties investigated, the only one that appeared to be constant throughout development was wall refractive index. This was determined according to equation (8). As shown in Text-fig. 3, the values fluctuated between 1.52 and 1.57, with very few exceptions. Rather than incorporate these apparently random fluctuations into wall thickness data, the mean value of 1.54 was used to calculate wall optical thickness after equation (6).

Another generalization to be made about the *Nitella* wall development is that, from the time birefringence first appears, its sign is always negative. This indicates that the birefringent material—probably cellulose—is arranged in crystalline units which have their long axes more or less at right

angles to the long axis of the cell, a condition common in many growing cell walls.

During wall development both retardation and wall optical thickness follow characteristic curves (Text-figs. 5 to 10). The ratio of these variables, R/T (Text-figs. 4, and 5 to 10), while changing less rapidly, is not constant. Variability in the value R/T reflects variation in the percentage of birefringent material or its orientation, or both. On the condition (not investigated) that the percentage of birefringent material be constant during development, R/T would be proportional to wall birefringence.

Stages of Development.—Once formed through the activity of the apical and segment cells, the internodal cell begins its enormous elongation and surface expansion. Two events during the growth of the wall, the attainment of the maximum relative elongation rate and the cessation of elongation, are sharply reflected in the structure of the wall. The course of growth will be briefly described. Because of the great range in cell length (3,000-fold), a plot of cell length against cell number is practical only for the larger cells (upper graphs, Text-figs. 5 to 10). In Text-fig. 2 the natural logarithm of cell length is plotted against cell number; beside the logarithms stand some corresponding values of absolute length. The abscissa can be considered a time axis if cell number is multiplied by 3 days. It is seen that cell elongation is characterized by a central phase of nearly steady logarithmic elongation; the relation between the start of this phase and cell number varies from plant to plant. For this reason it is advantageous to examine records from individual shoots in which the growth rate data is combined with the optical data from the same shoot (Test-figs. 5 to 10). Each record consists of two upper curves of cell length, L, and growth rate, $G.R.$, (the relative plastochron elongation rate after equation (5)) and three lower curves of optical properties. All are plotted against cell number. The apical cell is given number zero; the segment cell, when present, is given number one-half. The wall character of the apical, segment, and internodal cells will now be described.

The apical cell is hemispherical and has a wall optical thickness of 0.35 to 0.55 microns. The wall is isotropic in polarized light (Fig. 1 *a*), but this is probably not due to the absence of cellulose because microfibrils can be recognized on the inner surface of the wall (Fig. 3). These fibrils appear scattered at random. The faint negative birefringence seen in living apical cells (2) can be attributed to the curvature of the wall in the living state, in contrast to its flatness in the present preparations.

The segment cell, when present, is a cylindrical cell of about the same thickness as the apical cell and it is also isotropic. As mentioned above, the segment cell divides so that its upper portion forms a pro-node cell and its lower portion forms an internodal cell (Text-fig. 1). Before this division occurs, the inner surface of the upper part of the wall shows more or less regular indentations, a pattern which was found characteristic of certain node structures present (probably leaf bases). Figs. 10 to 12 show changes in the size and pattern of these indentations in three successively older nodes. These indentations appear to increase in size and to move farther apart as the leaf base expands. While this node-like structure is apparent in the upper part of the segment cell, the lower part has a structure intermediate between that of the apical cell and that of a typical internodal cell. The boundary between the two types of surfaces of the segment cell wall was diffuse.

The most recently formed internodal cells are numbers 1, 2, 3, (or 1½, 2½, 3½) in Text-figs. 5 to 10. In these diagrams it is seen that increase in cell number is associated with an increase in wall optical thickness (mass per unit area) until a peak value is reached approximately by cell number 3. During the same period retardation has increased from zero to a similar peak value. In the record of Text-fig. 10 it is seen that the peak in both wall optical thickness and retardation can be reached as early as cell number 1½. The peak in retardation of the more apical internodes is visible qualitatively in Fig. 1 *a*. These small cells of increasing thickness and retardation show near parallel microfibrils running transversely at the inner surface of the wall (Fig. 4).

The next older internode, typically number 3½ or 4, usually shows a much thinner wall and less retardation. These decreases may amount to 50 per cent. Note the drop in retardation in Fig. 1 *a*, center. The decreases in optical thickness and retardation are almost in proportion; hence their quotient changes considerably less (Text-fig. 4). It appears that the drop in wall optical thickness is correlated with the attainment of the maximum relative rate of elongation found in cell development. The maximum relative rate per plastochron of about 2.0 is equivalent to an elongation of about

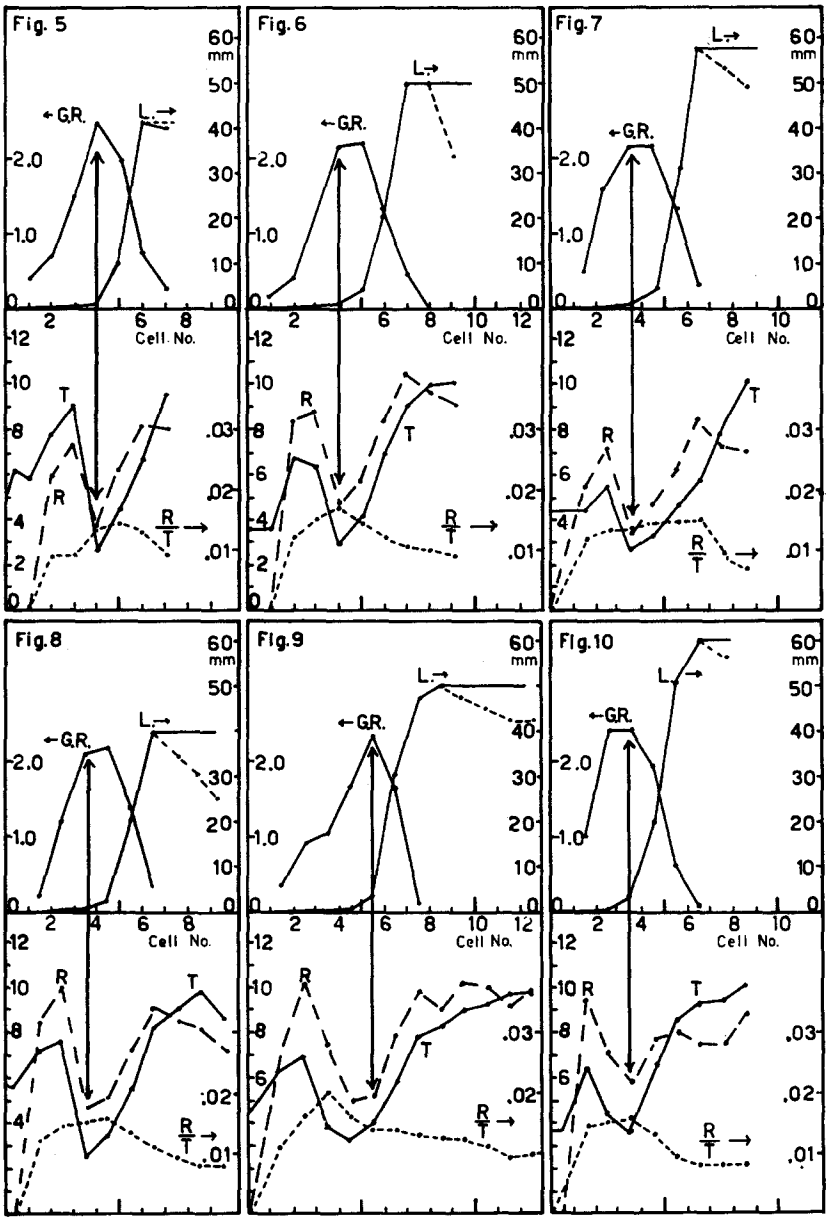

TEXT-FIGS. 5 to 10. Six similar records of growth and wall structure data; each record is from a single shoot. All curves are plotted against cell number as the abscissa. Cell number is equivalent to age when multiplied by 3 days. The two upper graphs in each record concern growth rate (*G.R.*), the relative rate of elongation per plastochron, and cell length (*L*). The scale for the growth rate is at the left, that for cell length at the right. The dashed line at the right of the cell length curves connects points from old cells that did not reach the maximum final cell length. Two of the lower three curves in each record, wall retardation (*R*) and wall optical thickness (*T*), use the scale at left. For retardation the scale stands for millimicrons. For wall optical thickness it stands for tenths of microns. The third of the lower curves, *R/T*, uses the scale at right.

2.8 per cent per hour. The correlation between maximum relative rate of elongation and minimum wall optical thickness is brought out by the six vertical arrows in Text-figs. 5 to 10. The inner surface of the wall shows microfibrils running mostly in the transverse direction, with very considerable scatter (Fig. 5). At times an irregular criss-cross pattern, perhaps similar to that described by Sterling and Spit (10) and Moor (11) for other cells, was observed.

Internodes approaching the end of their elongation, typically numbers 4 to 7, show a gradual increase in both wall optical thickness and retardation. These two variables do not increase in proportion; so the quotient, R/T, falls. The inner surface of such cells displays microfibrils dispersed as described above. When the end of elongation is at hand, the fibrils often appear better oriented and groups of near parallel fibrils are seen running in directions quite removed from the transverse. Such a surface, from a growing cell 60 mm. long, is given in Fig. 6. The continuous increase in wall optical thickness is well observed in Fig. 2, which show cells numbered 4 to 10.

Internodes which are no longer elongating (numbers greater than 6 or 7) do continue to form cell wall. Wall optical thickness increases, but there is no measurable increase in retardation. This indicates that an isotropic, or nearly isotropic, wall is being deposited. Examination of the inner surface shows a clear change in the microfibrillar pattern. The fibrils are present in fields of well ordered microfibrils, as in Fig. 7 and the background of Fig. 9. The direction of fibrils of a given field may bear any relation to the cell axis. The fields may partially overlap one another as in Fig. 7, or they may appear to merge with one another through a gradual curving of fibrils. The superposition of fields of microfibrils of different orientation thus leads to the deposition of an essentially isotropic wall after the cessation of elongation. The overlapping fields may be the basis for a faint crossed-striation pattern noticed in *Nitella* walls in 1893 by Correns (12). This isotropic wall deposited after elongation in *Nitella* stands in contrast with the corresponding (secondary) wall of higher plants which is usually highly birefringent.

Various unusual structures were observed in these non-elongating walls. Circular microfibrillar patterns (Fig. 9) were found as well as regions of radiating microfibrils (Fig. 8). These latter were found only on very old walls (number 10 or greater) and not on all of these. The radiating structures may be related to the cessation of cellulose formation by the cell. Some of the radiating fibrils appeared to merge, through bending, with the course of the background fibrils (Fig. 8, lower right). Somewhat similar structures were described by Preston *et al.* (13) for the inner wall surface of the *Valonia* vesicle, and it was felt that these might represent "islands of syntheses" of new microfibrils. Macerated cambium cells also yielded apparent islands of synthesis (14). The present structures were found only in the oldest non-elongating walls and thus the view that they represent the typical sites of cellulose synthesis cannot be advanced for the *Nitella* cell wall.

Internodes of number greater than 10 or 11 had undergone part of their growth in a previous preparation of nutrient medium. They attained final cell lengths less than those cells which developed entirely in one preparation of medium. Thus data from these old cells cannot be considered strictly comparable with that from other cells. Therefore, their cell length is shown by dashed lines in the upper graphs of Text-figs. 5 to 10. In the case of Text-fig. 9, these old (more than a month) walls continued to show an increase in wall optical thickness. The exact age at which a cell no longer deposits cell wall has not been established.

DISCUSSION

The *Nitella* internodal cell wall, from the time its cylindrical form is first apparent, has negative birefringence and microfibrils disposed predominantly at right angles to the axis of the cell. This correlation between the fine structure of the wall and the direction of its growth is very widespread. Among lower plants, the large cylindrical cells of the alga *Hydrodictyon* have negative birefringence (15); the growth zone of the sporangiophore of the fungus *Phycomyces* is also negatively birefringent (16). Among higher plants this type of wall structure has been described for *Avena* coleoptile parenchyma, setae of the moss *Pellia*, the cambium, cambium derivatives (17) and many other cells, primarily on the basis of polarized light data; x-ray investigations have also indicated transverse arrangement of cellulose crystallites in bean internodes (18) and other tissues. Electron microscopic observations have confirmed the presence of a predominantly transverse arrangement of microfibrils in *Avena* coleoptile parenchyma (19, 20), the root meristem (21), etc. In a pair of important

papers Roelofsen and Houwink (22, 23) showed that in a variety of higher plant cells (staminal hairs, cotton fibers, stellate pith cells, etc.) not all the microfibrils were oriented in the transverse direction. This orientation prevailed at the inner surface of the wall, but the outer surfaces of these cells displayed microfibrils running longitudinally. The transverse fibrils would predominate, giving the negative birefringence. These authors put forth the multinet growth theory in which primary wall growth would take place through the deposition of transversely oriented microfibrils at the inner surface of the wall, while the elongation of the cell would tend to reorient the previously deposited, passive, outer microfibrils into an isotropic or longitudinal pattern. Other authors have found this theory to apply to other cell types, including *Avena* parenchyma (20). Because no fibrils are seen in replicas of the outer wall surface of *Nitella*, the theory has not been tested in this plant. The view that transverse fibrils are deposited probably exclusively at the inner surface of the wall does have experimental support in the case of *Nitella* (3). Previously the author had assumed microfibril formation took place inside the wall proper (2). To sum up, a wide variety of plant cells apparently show common features of primary wall structure: arrangement of cellulose crystallites at right angles to the direction of elongation.

This structure is, however, not universal for growing cells. The outer epidermal walls of *Helianthus* hypocotyls (15) and *Avena* coleoptiles (24) show a majority of the microfibrils in the longitudinal direction, the direction of growth. Ribs of longitudinal microfibrils are found in the negatively birefringent parenchyma of *Avena* coleoptiles (25). Positive birefringence is found in elongating collenchyma cells where a type of secondary wall is deposited before elongation has ceased (26). The typical growing wall structure, described above, was not found in the elongating fiber cells of *Asparagus* by Sterling and Spit (10). They found no exact correlation between fibrillar orientation and the direction of elongation, but found that the wall possessed two crossing systems of near parallel microfibrils. Each set made an angle of more than 45° with the cell axis in accord with the negative birefringence of these cells. Moor (11) found a similar structure in the wall of the latex tube of *Euphorbia* where thin lamellae of alternating sign of helical microfibrillar orientation were deposited interior to the first formed isotropic wall. The latex tube increased in both length and breadth while achieving this structure. The crossed helical systems do not quite compensate and give a negative birefringence. Thus there is no universal primary wall structure in higher plants, but negative birefringence is almost universal.

A very great variety of green algae were investigated with x-ray diffraction methods by Nicolai and Preston (27), and it appears that among the algae there are a great many forms with wall structures different from those of higher plants. In the broad survey of Nicolai and Preston, no precise correlations between growth rates and wall structure were made, this being beyond the scope of an already large project. Their diagrams came from bundles of algal filaments (100 filaments for *Stigeoclonium*), and it was not clear what fraction of the cells which gave rise to the diagram were in the act of growing. It is possible that such samples might contain cells in all stages of development, perhaps the majority of them mature.

These workers found three general types of green algal cell wall. Only the first group contained cellulose of the type found in higher plants (cellulose I) and this was present in a crossed-fibrillar pattern. The wall consisted of many lamellae of parallel microfibrils, the direction of the fibrils being nearly transverse to the cell axis for about half the lamellae, nearly longitudinal for the rest. The result is that the wall is only weakly birefringent due to mutual compensation by the two chain systems. This structure was described for *Cladophora*, *Siphonocladus*, *Dictyosphaeria*, and other genera. It had previously been described for the barrel-shaped cells of *Chaetomorpha* (28) and the vesicles of *Valonia* (26). Nicolai and Preston (27) investigated a young *Cladophora* plant and found that the longitudinal set of cellulose chains predominated; in older plants the transverse set usually predominated. Observations on similar material with polarized light showed the young cells to be isotropic, older cells negatively birefringent. Ziegenspeck (29) had found the growing cells to be optically negative. These optical observations are generally similar to those described for developing *Nitella* (and higher plant) cells.

A very different wall structure was found by Nicolai and Preston in their second group of green algae. Here the interplanar spacings indicated that the cellulose present was of a different crystalline type, that of mercerized cellulose (cellulose

II) or a derivative. Further, there was commonly no sign of orientation with respect to any morphological axis. This was found for bundles from such genera as *Ulothrix*, *Stigeoclonium*, *Spongomorpha*, *Monostroma*, and *Hydrodictyon*. A random arrangement of crystallites in cells of cylindrical shape is unexpected. For the case of *Hydrodictyon* one would expect some orientation because the wall is negatively birefringent (15). Perhaps some of the randomness of orientation stems from the fact that the bundles would present the x-ray beam with a great variety of wall positions (face view, end view, and all intermediates), and this would obscure some structural detail.

The third group of algae, which included *Nitella*, contained forms in which the major wall constituent was apparently not cellulose. In some filamentous species there was some orientation (arcs either on the equator or meridian of the diagram, as in *Spirogyra* and *Vaucheria*); in others there was none despite the presence of a well crystallized substance (*Enteromorpha*). In other filamentous forms including *Zygnema*, *Bryopsis*, *Chara*, and *Nitella* the diagram was too diffuse to permit any interpretation. The *Nitella* wall has been shown to contain a substance giving the staining reactions of cellulose (12, 30), and its microfibrillar and birefringent character have been described above for all stages of development. It is possible that the birefringent material is present in crystallites too small to give arc diffraction. The interference of non-cellulosic substances can apparently modify or obliterate the x-ray diagram (31), sometimes rendering negative findings on untreated material of limited value. In the absence of detailed growth-structure studies on many of the algae it is perhaps too early to express the view that no underlying connection between cell form and cell wall fine structure exists (26), but it is clear that such a connection, while apparent in higher plants and *Nitella*, is not apparent in the majority of algal species.

The somewhat recent application of interference microscopy to biology (32, 33) has permitted the first accurate estimation of wall optical thickness in the typically thin primary cell wall. It is seen in Text-figs. 5 to 10 that wall optical thickness reaches a peak value when the cell is small, then drops suddenly as the cell attains its maximum relative rate of elongation, then gradually increases again as the cell elongates to its final length. Earlier observations have been made on the absolute thickness of elongating cells. If the degree of wall swelling is constant during elongation, absolute wall thickness will be proportional to optical thickness. In *Helianthus* hypocotyls Diehl *et al.* (15) found wall thickness to decrease, then increase again during elongation. The increase in elasticity characteristic of Burström's first phase of root cell elongation (34, 35) may also reflect a temporary drop in wall thickness. While in the above cases wall thickness increases after an early dip, as in *Nitella*, in other plants wall thickness apparently decreases continuously during elongation. Preston and Clark (36), studying wall growth in intact *Avena* coleoptiles, found that wall material per coleoptile increased steadily during elongation but the increase in surface area was even more rapid, giving a net decrease in wall thickness during elongation. A similar condition is found in the setae of the moss *Pellia* (37). The continuous increase in wall optical thickness during the bulk of *Nitella* internode elongation (5 mm. to 50 to 60 mm.) stands in contrast to these latter observations.

Ruge (38), studying *Helianthus* hypocotyls, measured the retardation of the cell walls and found that the application of growth-substance caused the walls to retard less and less during the start of elongation; then retardation increased again. A dip, then rise, of retardation is characteristic for *Nitella*. Maas Geesteranus (39) made compensator readings on the developing arms of *Juncus* stellate pith cells and found, in the manner of *Nitella* internodes number 4 to 10, an increase in retardation with increase in arm length.

The wall structure of *Nitella* node cells (Figs. 10 to 12) bears a superficial resemblance to primary pit membranes (40) but, since this structure appears to exist in regions other than cell contacts (the cylindrical wall of the sement cell), it should be considered an unusual wall type.

The older cell wall literature is reviewed by Küster (41); electron microscopical investigations of cell wall structure have recently been reviewed by Frey-Wyssling (42, 43) and Mühlethaler (44, 45).

During the present investigation the writer held a Junior Fellowship from Harvard University which enabled him to carry out research at the Institute of General Botany, The Swiss Federal Institute of Technology, Zurich, Switzerland. The kindness and help of his hosts, Professors Frey-Wyssling, Mühlethaler, and Ruch are gratefully acknowledged.

BIBLIOGRAPHY

1. Frey-Wyssling, A., Submicroscopic Morphology of Protoplasm, Amsterdam, The Elsevier Press, Inc., 1953.
2. Green, P. B., and Chapman, G. B., *Am. J. Bot.*, 1955, **42,** 685.
3. Green, P. B., *Am. J. Bot.*, 1958, **45,** in press.
4. Fritsch, F. E., The Structure and Reproduction of the Algae, New York, The Macmillan Co., 1935.
5. Green, P. B., *Am. J. Bot.*, 1954, **41,** 403.
6. Askenasy, E., *Verh. naturh.-med. Ver. Heidelberg,* 1880, **2,** 70.
7. ERICKSON, R. O., and Michelini, F. J., *Am. J. Bot*, 1957, **44,** 297.
8. Milne, W. E., Numerical Calculus, Princeton, New Jersey, Princeton University Press, 1949.
9. Barer, R., The interference microscope, *in* Quantitative Cytology, London, C. Baker of Holborn, Ltd., 1956.
10. Sterling, C., and Spit, B. J., *Am. J. Bot.*, 1957, **44,** 851.
11. Moor, H., Feinbau der Milchroehren, Diplomarbeit der Eidgenössischen Technischen Hochschule, Zürich, 1956.
12. Correns, C., *Zimmermann's Beitr. Morphol. u. Physiol. Pflanzenz.*, 1893, **1,** 260.
13. Preston, R. D., Nicolai, E., and Kuyper, B., *J. Exp. Bot.*, 1953, **4,** 40.
14. Preston, R. D. and Ripley, G. W., *J. Exp. Bot.*, 1954, **5,** 410.
15. Diehl, J. M., Gorter, C. J., van Iterson, Jr., G., and Kleinhoonte, A., *Rec. trav. bot. néerl.*, 1939, **36,** 709.
16. Castle, E. S., *Protoplasma,* 1938, **31,** 331.
17. Frey-Wyssling, A., Submicroscopic Morphology of Protoplasm and its Derivatives, Amsterdam, The Elsevier Publishing Co., 1948.
18. Williams, W. T., Preston, R. D., and Ripley, G. W., *J. Exp. Bot.*, 1955, **6,** 451.
19. Wardrop, A. B., *Australian J. Bot.*, 1955, **3,** 137.
20. Wardrop, A. B., *Australian J. Bot.*, 1956, **4,** 193.
21. Scott, F. M., Hamner, K. C., Baker, E., and Bowler, E., *Am. J. Bot.* 1956, **43,** 313.
22. Roelofsen, P. A., and Houwink, A. L., *Acta Bot. Néerl.*, 1953, **2,** 218.
23. Houwink, A. L., and Roelofsen, P. A., *Acta Bot. Néerl.*, 1954, **3,** 385.
24. Bayley, S. T., Colvin, J. R., Cooper, F. P., and Martin-Smith, C. A., *J. Biophysic. and Biochem. Cytol.*, 1957, **3,** 171.
25. Mühlethaler, K., *Z. Zellforsch.*, 1953, **38,** 299.
26. Preston, R. D., The Molecular Architecture of Plant Cell Walls, London, Chapman and Hall, Ltd., 1952.
27. Nicolai, E., and Preston, R. D., *Proc. Roy. Soc. London, Series B,* 1952, **140,** 244.
28. Nicolai, E., and Frey-Wyssling, A., *Protoplasma,* 1938, **30,** 401.
29. Ziegenspeck, H., *Protoplasma,* 1939, **32,** 342.
30. Votava, A., *Oesterr. Bot. Z.*, 1914, **64,** 442.
31. Nicolai, E., and Preston, R. D., *Nature,* 1953, **171,** 752.
32. Davies, H. G., Wilkens, M., Chayen, J., and La Cour, F., *Quart. J. Micr. Sc.*, 1954, **95,** 271.
33. Barer, R., *J. Opt. Soc. America,* 1957, **47,** 545.
34. Burström, H., *Ann. Agric. Coll. Sweden,* 1942, **10,** 1.
35. Frey-Wyssling, A., Deformation and Flow in Biological Systems, Amsterdam, North-Holland Publishing Co., 1952.
36. Preston, R. D. and Clark, C. S., *Proc. Leeds Phil. and Lit. Soc., Sc. Sect.*, 1944, **4,** 201.
37. Overbeck, F., *Z. Bot.*, 1934, **27,** 129.
38. Ruge, U., *Z. Bot.*, 1937, **31,** 1.
39. Maas Geesteranus, R. A., *Nederl. Akad. Wetensch.*, 1941, **44,** 489.
40. Frey-Wyssling, A., and Müller, H. R., *J. Ultrastruct. Research,* 1957, **1,** 38.
41. Küster, E., Die Pflanzenzelle, Jena, Gustav Fischer Verlag, 1956.
42. Frey-Wyssling, A., Macromolecules in Cell Structure, Cambridge, Massachusetts, Harvard University Press, 1957.
43. Frey-Wyssling, A., Die Pflanzliche Zellwand, Berlin, Springer-Verlag, 1958, in press.
44. Mühlethaler, K., *Z. Zellforsch.*, 1953, **38,** 299.
45. Mühlethaler, K., Plant cell walls, *in* The Cell, New York, Academic Press, Inc., 1958, in press.

Explanation of Plates

Plate 247

Fig. 1 *a*. A "quartered" *Nitella* shoot apex photographed between crossed polarizing prisms. The successive bright areas are single thicknesses of internodal cell wall. The darker areas in between are nodes from which the laterals have been removed. The brightness of the two uppermost internodal cell walls, compared with the two below, reflects a greater wall optical thickness in the smaller cells. A segment cell and apical cell at the tip of the shoot are isotropic and appear dark. × 20.

Fig. 1 *b*. The apical tip of a "quartered" apex in the interference microscope. Note that the single thicknesses of apical and segment cell wall shift the dark band slightly to the left. × 160.

Fig. 2. A series of segments of internodal cell wall (horizontal bands) in the interference microscope. At extreme top and bottom are the vertical interference bands of the field. Beginning above with a piece of wall from a cell of number 4, each wall segment is from a cell 3 days older than the one above. The progressive shift of the interference bands to the left reflects a progressive increase in wall optical thickness (mass per unit area).

Figs. 3 to 6. Electron microscope pictures of replicas. The black bar at right is equivalent to a distance of one micron on the original replica. The cell axis is equivalent to the long edge of the page.

Fig. 3. The inner surface of the apical cell. Thinly scattered microfibrils are seen disposed at random in the plane of the wall inner surface. × 28,000.

Fig. 4. The inner surface of a small (length 110 microns) internodal cell wall. The microfibrils appear well ordered and run at right angles to the cell axis. × 28,000.

Fig. 5. The inner surface of a longer (10 mm.) internodal cell wall. The fibrils are scattered about a preferred direction at right angles to the cell axis. Some near parallel fibrils are seen running in a helical direction in a plane below that of the surface fibrils. × 20,000.

Fig. 6. The inner surface of a very long (60 mm.) internodal cell wall about to cease elongating. Note groups of microfibrils running in directions different from the transverse. × 17,000.

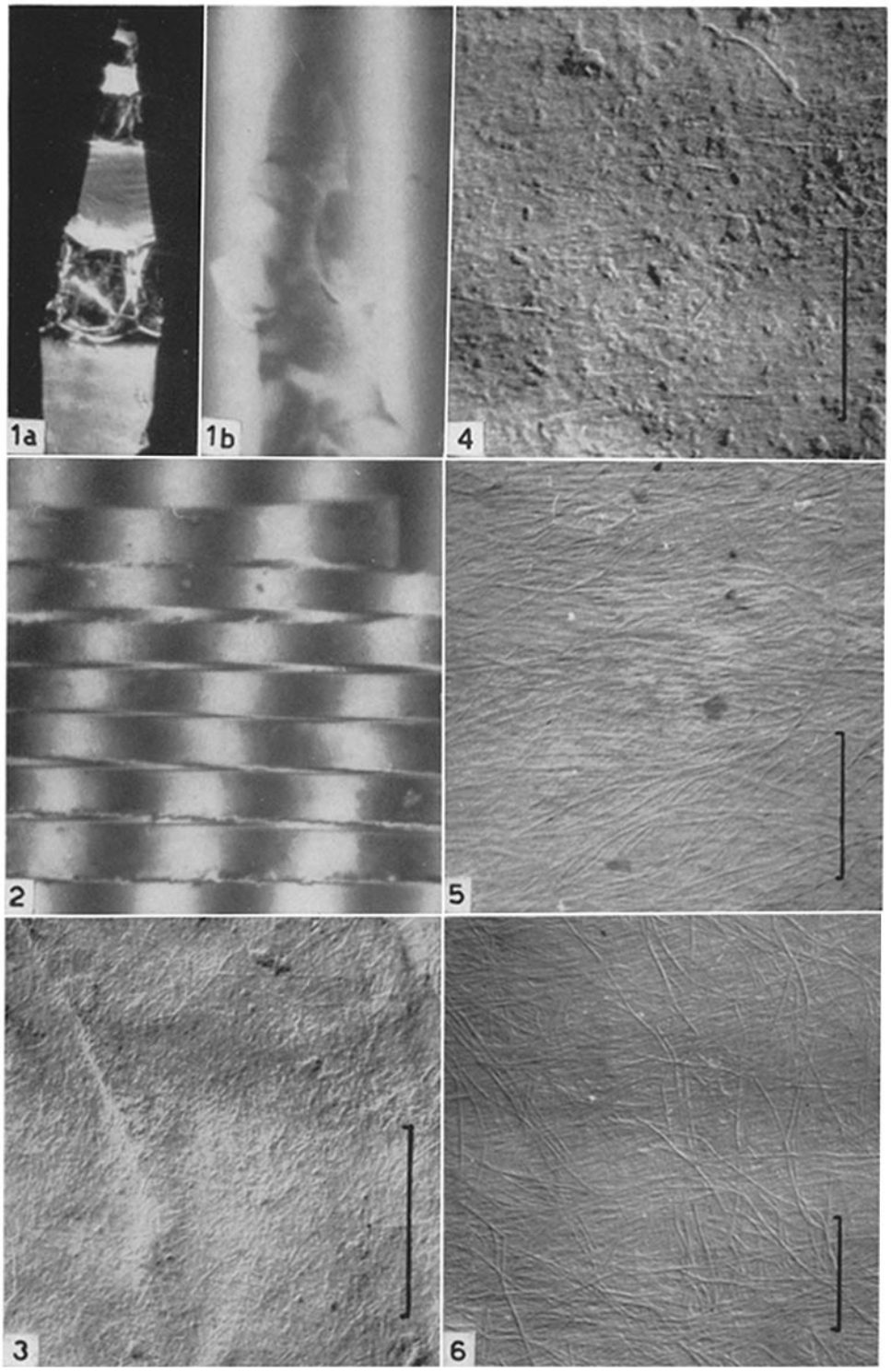

(Green: Structure of developing *Nitella* cells)

PLATE 248

FIGS. 7 to 12. Electron micrographs of replicas of the inner surfaces of *Nitella* cell walls. The black bar at right is equivalent to a distance of one micron on the original replica.

FIG. 7. The inner surface of an internodal cell wall that has ceased elongating. The microfibrils occur in fields which appear to partially overlap one another. × 20,000.

FIG. 8. A group of radiating microfibrils seen on the inner surface of an internode cell wall that has ceased elongating. At the lower right, the fibrils appear to bend to assume the direction of the underlying fibrils. × 13,000.

FIG. 9. Two circular patterns of microfibrils seen on the inner surface of an internode cell wall that has ceased elongating. × 15,000.

FIGS. 10 to 12. The inner surfaces of cell walls that are parts of nodes.

FIG. 10. Node tissue below internodal cell number 1. × 28,000.

FIG. 11. Node tissue below internodal cell number 2. × 28,000.

FIG. 12. Node tissue below internodal cell number 3. × 28,000.

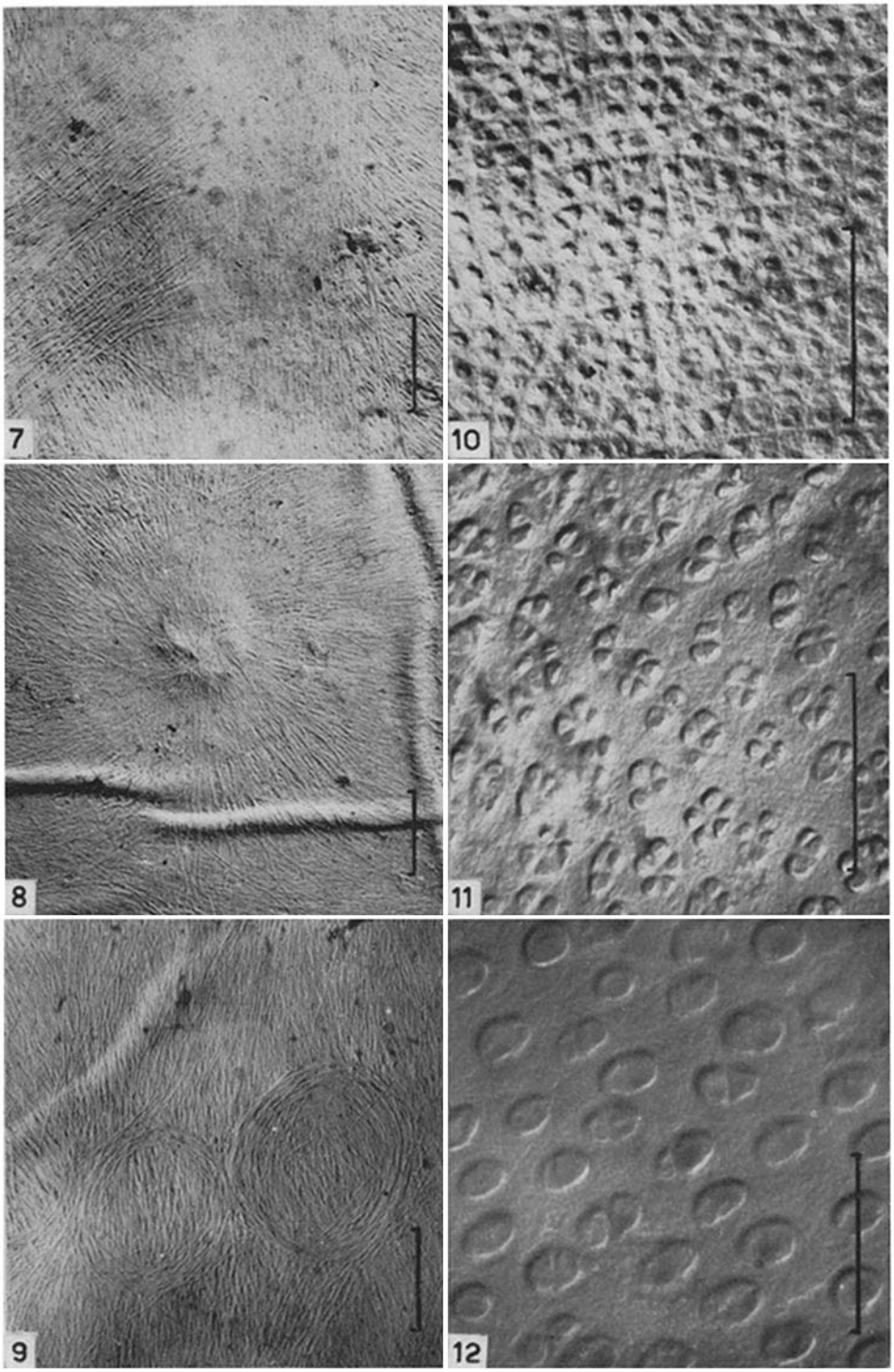

(Green: Structure of developing *Nitella* cells)